S passivation of GaAs and band bending reduction upon atomic layer deposition of HfO_2/Al_2O_3 nanolaminates

F. S. Aguirre-Tostado,[1,a)] M. Milojevic,[1] K. J. Choi,[1] H. C. Kim,[1] C. L. Hinkle,[1] E. M. Vogel,[1] J. Kim,[1] T. Yang,[2] Y. Xuan,[2] P. D. Ye,[2] and R. M. Wallace[1,b)]
[1]*Materials Science and Engineering, The University of Texas at Dallas, Richardson, Texas 75083, USA*
[2]*School of Electrical and Computer Engineering and Birck Nanotechnology Center, Purdue University, West Lafayette, Indiana 47907, USA*

(Received 11 April 2008; accepted 1 July 2008; published online 13 August 2008)

A systematic study of the interface engineering and dielectric properties of nanolaminated hafnium aluminate on GaAs is presented. The dielectrics were deposited using atomic layer deposition of alternating cycles of HfO_2 and Al_2O_3 on GaAs substrates. High resolution x-ray photoelectron spectroscopy (XPS) showed differences in space charge amounts at the interface for the two surface treatments [NH_4OH or $(NH_4)_2S$]. *In-situ* XPS analysis shows that chemical bonding to oxygen across the nanolaminate film is independent of the interface formation conditions. In addition, the GaAs surface treated with $(NH_4)_2S$ shows a decreased band bending and slightly thinner films with respect to NH_4OH. © *2008 American Institute of Physics*. [DOI: 10.1063/1.2961003]

The search for an appropriate high-κ dielectric on GaAs for scaled metal-oxide-semiconductor (MOS) device applications with an ideal semiconductor/dielectric interface remains a challenge. Both dielectric and GaAs/dielectric interface quality play a key role on the electrical performance of GaAs based MOS devices.[1–3] Although tremendous progress has been attained[3,4] in regard to interface passivation and dielectric properties, the need for a manufacturable, high throughput process limits the possibilities. The use of deposition techniques such as atomic layer deposition (ALD) and *ex-situ* GaAs surface preparation is preferable. Recent studies have demonstrated that ALD grown Al_2O_3 shows reduced leakage current with respect to HfO_2 while the latter possess a larger dielectric constant. In previous work,[5] it has been demonstrated that nanolaminated films of Al_2O_3/HfO_2 show better scalability than Al_2O_3 as well as lower leakage and higher breakdown than in HfO_2. In addition, the chemical bonding arrangement at the interface in GaAs resulted critical for the removal of the "frequency dispersion" phenomenon.[6–8] It is also known that the interface bonding arrangement is modified during the initial ALD, where the main chemisorption mechanisms,[9] "ligand exchange" and "dissociation," could be responsible for the reduction ("self-cleaning") of GaAs surface oxides. In a previous study, it was also found that this interfacial self-cleaning is precursor dependent as well as oxidation state dependent.[10]

The passivation of surface states in silicon resulting in midgap interface state densities on the order of $10^{10}/cm^2$ eV can be achieved with the use of thermally grown SiO_2, the native oxide of Si. In contrast, the GaAs native oxide, which is composed mainly of Ga_2O_3, As_2O_5, and As_2O_3, is known to produce a relatively poor interface and Fermi level pinning.[11,12] During the last two decades, the use of sulfide solutions have proven to passivate the GaAs surface.[13–15] Experimental and theoretical studies[16–19] have shown that the passivation of GaAs using ammonium sulfide solutions [$(NH_4)_2S$ or $(NH_4)_2S_x$] results in Ga–S and As–S bonds that provide protection against further oxidation. Recent studies have examined the effect of NH_4OH and $(NH_4)_2S$ surface treatments[20,21] on ALD Al_2O_3 on GaAs, where previous reports of surface oxide reduction were reaffirmed.[22,23] In this letter, we present a high resolution x-ray photoelectron spectroscopy (XPS) study of *nanolaminated* HfO_2/Al_2O_3 dielectrics deposited by ALD on GaAs chemically treated with either NH_4OH or $(NH_4)_2S$ and with two different starting layers (Al_2O_3 or HfO_2).

Two samples employed were, *ex-situ* ALD grown Al_2O_3/HfO_2 nanolaminates and *in-situ* HfO_2 films grown on *n*-type (Si: 5×10^{-17} cm^{-3}) GaAs(001) substrates. In the case of the *ex-situ* samples, the Al_2O_3/HfO_2 nanolaminates were 3 nm thick and grown by ALD starting with either five ALD cycles of Al_2O_3 (using trimethyl aluminum and water) or HfO_2 (using $HfCl_4$ and water). Prior to ALD, the substrates were cleaned by a degreasing[5] step followed by an etch in either 3 min in 29% NH_4OH or 1 min in 29% $HCl:H_2O$ (1:1) plus 10 min in 22% $(NH_4)_2S$. The ALD was carried out at 300 °C in an ASM F-120 ALD module. After the five ALD cycles of either Al_2O_3 or HfO_2 serving as a template initiation layer, the overlying nanolaminated layer structure contained alternate layers of Al_2O_3 (one cycle) and HfO_2 (two cycles). The *in-situ* HfO_2 films were deposited in a *Picosun* ALD chamber connected to the XPS analysis chamber through a UHV transfer chamber. The HfO_2 was deposited on NH_4OH and $(NH_4)_2S$ treated *n*-type GaAs using ten cycles of tetraethyl-methyl-amino-Hf (TEMA-Hf) and water to form 1 nm thick films. The analysis was carried out in an *Omicron* XPS system using a monochromatic Al $K\alpha$ x-ray source ($h\nu=1486.7$ eV and 0.25 eV line width) and a hemispherical analyzer equipped with seven Channeltrons®.

Figure 1(a) shows the O 1*s* spectra for a 3 nm thick HfO_2/Al_2O_3. All the O 1*s* regions were aligned in binding energy (BE) to the Hf–O–Al peak at 531.5 eV to allow for better comparison. After a peak shift the line shape of the O 1*s* spectra for the four samples [see Fig. 1(a)] are identical. This suggests that the oxygen chemical state in the Al_2O_3/HfO_2 nanolaminates for the two different surface

a)Electronic mail: servando@utdallas.edu.
b)Electronic mail: rmwallace@utdallas.edu.

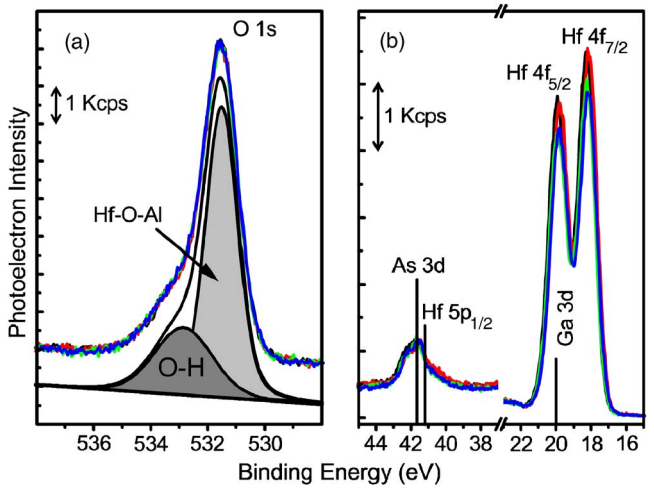

FIG. 1. (Color online) (a) Aligned XPS regions for O 1*s* show no differences in the line shape. Peak fitting shows only two chemical components for oxygen, one associated with O–H bonds from air exposure and the other associated with Hf–O–Al. (b) Raw XPS region showing Hf 4*f*, Hf 5*p*, Ga 3*d*, and As 3*d* core levels.

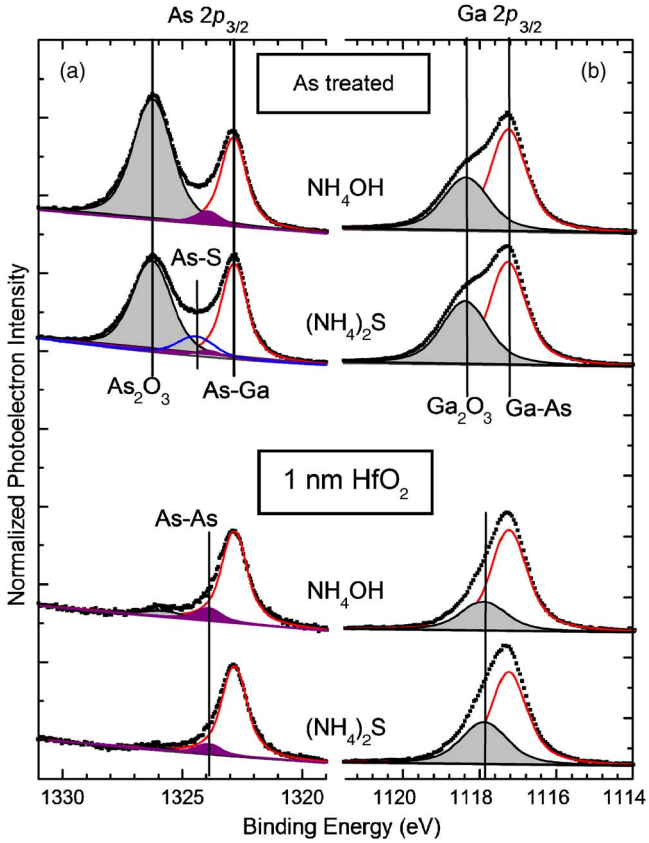

FIG. 2. (Color online) Ga 3*d* and Hf 4*f* (a) after the chemical cleaning in either NH_4OH or $(NH_4)_2S$ and (b) after the ALD of 1 nm of HfO_2 *in-situ*. The fits shown are for the NH_4OH treated GaAs.

treatments and the two different starting layers are similar. Figure 1(b) shows the regions for Hf 4*f* and Ga 3*d*, and Hf 5*p* and As 3*d* core levels. Hf 4*f* shows a similar Gaussian width in all the films, but the intensity is slightly larger for the samples initiated with HfO_2. All core levels in the film and substrate show a synchronous BE shift of 0.11 ± 0.02 eV to lower BE for the nanolaminates deposited on GaAs treated with NH_4OH with respect to $(NH_4)_2S$. Similar XPS BE shifts have been found by other authors for S-passivated GaAs surfaces.[24] This synchronous shift is interpreted in terms of a GaAs band bending increase for the surface treated with NH_4OH as will be discussed below.

Due to the overlapping of the Ga 3*d* and As 3*d* with Hf peaks, as shown in Fig. 1(b), it is not possible to resolve the remaining Ga and As oxides at the interface. With the purpose of minimizing the attenuation of the signal coming from the interface, 1 nm thick HfO_2 ALD films were grown *in-situ* on GaAs with the two different surface treatments.

Figure 2 shows the (a) As 2*p* and (b) Ga 2*p* core level spectra before and after the deposition of HfO_2. *In-situ* ALD experiments using 1 nm of Al_2O_3 show similar results (data not shown). The effective attenuation lengths for As 2*p* and Ga 2*p* photoelectrons, which are 8 and 12 Å, respectively,[25] allow for better surface sensitivity. The initial NH_4OH "as-treated" GaAs surface shows As_2O_3, elemental As, and Ga_2O_3. The $(NH_4)_2S$ treated surface show the same chemical species with an additional As peak at 1.58 eV above the As-bulk component, which is associated to As–S bonds.[17] The Ga 2*p* component for the $(NH_4)_2S$ treated surface contains Ga–O and Ga–S bonds, however due to its Gaussian width (0.99 eV) it is not possible to resolve these. However it is noted that Ga–O peak intensity for the $(NH_4)_2S$ treated GaAs is larger than for the NH_4OH treated surface.

After the ALD deposition of 1 nm thick HfO_2, the As–O and As–S bonds are substantially reduced while the amount of As–As bonds are nearly unchanged. Ga–O separation with respect to the Ga-bulk peak (Ga–As) is decreased from 1.11 to 0.65 eV. In addition the Ga–O intensity is reduced to a lesser extent than the As–O bond. The Ga–O peak intensity is again slightly larger for the sample that was treated with $(NH_4)_2S$, and this could be due to the remaining Ga–S bonds that are nonexistent in the NH_4OH treated sample. Previous synchrotron radiation studies with extremely high surface sensitivity reported a Ga–S chemical shift of 0.55 eV and have shown that 400 °C anneals will convert As–S to Ga–S bonds.[17,26] The increased Ga–O peak [shaded peak in Fig. 2(b)] after 1 nm HfO_2 ALD deposition at 300 °C for the $(NH_4)_2S$ with respect to the NH_4OH treatment suggests the presence of a Ga–S peak whose BE is close to that of the Ga–O peak. Regardless of the coexistence of Ga–O and Ga–S bonds for the S-treated surface before and after the HfO_2 growth, the overall drop in the intensity of Ga–O and Ga–S witnesses, to some extent, a self-cleaning effect[10] for S-passivated GaAs surfaces.

The Ga 3*d* and Hf 4*f* XPS spectra are shown in Fig. 3. The initial as-treated GaAs surfaces show Ga 3*d* peaks at the same BE [see Fig. 3(a)]. After the ALD of 1 nm of HfO_2 at 300 °C, all the peaks for the NH_4OH treated surface suffer a synchronous shift to lower BE of 0.11 ± 0.02 eV. It is also observed that the Hf 4*f* peak intensity for the $(NH_4)_2S$ treated surface is smaller. This suggests that the HfO_2 nucleation at the early stage of the ALD growth is favored for the NH_4OH treated surface with respect to the $(NH_4)_2S$ treated, and may be evidence of surface chemical passivation for the sulfur-treated surface as far as the ALD process is concerned. The surface treatment-dependent BE shift obtained from the Hf 4*f* feature is plotted in Fig. 3(c). All other core level spectra acquired show a similar BE shift in the same direction. This collective BE shift can be only explained by a reduction in the semiconductor band bending for the surfaces

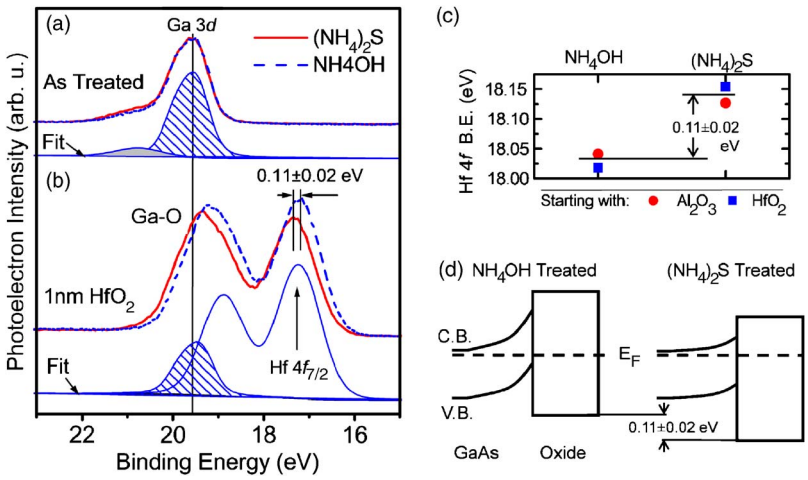

FIG. 3. (Color online) Ga 3*d* and Hf 4*f* (a) before and (b) after the ALD of 1 nm of HfO_2 *in-situ*. The as-treated surfaces show Ga 3*d* peaks at the same BE position while there is a shift of 0.11 ± 0.02 eV to lower BE for the NH_4OH treated surface after the HfO_2 deposition. (c) BE shift of Hf 4*f* core levels for the samples treated with $(NH_4)_2S$ with respect to those treated with NH_4OH. (d) Corresponding band diagram showing band bending reduction for the S-passivated *n*-type GaAs.

treated with $(NH_4)_2S$ with respect to the one treated with NH_4OH. The BE shift difference between the two surface treatments has been observed in four different samples deposited *in-situ* and *ex-situ*. The BE shift between the surface treatments cannot be interpreted as sample charging differences because the substrates used are the same. We note that in the event of charging, a shift toward higher BE is expected for the sample treated with NH_4OH because the associated ALD film grown on this surface treatment is slightly thicker. As indicated in Fig. 3, we observe the opposite behavior.

Figure 3(d) depicts an oxide/semiconductor interface band diagram showing the effect of band bending reduction for the S-passivated surface. The increase of interface space charge for the NH_4OH treated surface results in additional band bending to compensate the charge present at the interface. The electronic structure of the oxide/semiconductor shifts up with respect to the Fermi level causing a reduction in the measured BE. The same BE shift is observed for the *in-situ* 1 nm thick HfO_2 as well as for the *ex-situ* grown 3 nm thick HfO_2/Al_2O_3 nanolaminate regardless of the starting template. These observations demonstrate the prevalence of S-passivation from the $(NH_4)_2S$ surface treatment of GaAs.

In conclusion, XPS analysis shows the same chemical bonding arrangement of oxygen in the HfO_2/Al_2O_3 nanolaminate regardless of the surface treatment or the starting layer (HfO_2 or Al_2O_3). A self-cleaning effect was found for both $(NH_4)_2S$ and NH_4OH GaAs surface treatments upon the ALD deposition of HfO_2. A systematic BE shift of 0.11 ± 0.02 eV to higher energies for the S-passivated surfaces and is interpreted as a decrease in band bending due to the reduction of interfacial space charge. Although sulfur is below the XPS detection limit, these results suggest that some amount of sulfur may remain at the oxide/semiconductor interface after the ALD growth at 300 °C.

This work is supported by the MARCO Focus Center on Materials, Structures, and Devices, the National Institute of Standards and Technology, Semiconductor Electronics Division, and FUSION (by COSAR, Korea).

[1]C. W. Wilmsen, *Physics and Chemistry of III-V Compound Semiconductor Interfaces* (Plenum, New York, 1985).
[2]M. Passlack, Proceedings of the Electrochemical Society, 2005 (unpublished), Vol. PV 2005-01, pp. 417–433
[3]M. Passlack, M. Hong, and J. P. Mannaerts, Appl. Phys. Lett. **68**, 1099 (1996).
[4]H. C. Lin, P. D. Ye, and G. D. Wilk, Appl. Phys. Lett. **87**, 182904 (2005).
[5]T. Yang, Y. Xuan, D. Zemlyanov, T. Shen, Y. Q. Wu, J. M. Woodall, P. D. Ye, F. S. Aguirre-Tostado, M. Milojevic, S. McDonnell, and R. M. Wallace, Appl. Phys. Lett. **91**, 142122 (2007).
[6]C. L. Hinkle, A. M. Sonnet, E. M. Vogel, S. McDonnell, G. J. Hughes, M. Milojevic, B. Lee, F. S. Aguirre-Tostado, K. J. Choi, J. Kim, and R. M. Wallace, Appl. Phys. Lett. **91**, 163512 (2007).
[7]S. Oktyabrsky, V. Tokranov, M. Yakimov, R. Moore, S. Koveshnikov, W. Tsai, F. Zhu, and J. C. Lee, Mater. Sci. Eng., B **135**, 272 (2006).
[8]I. Ok, H. Kim, M. Zhang, C.-Y. Kang, S. J. Rhee, C. Choi, S. A. Krishnan, T. Lee, F. Zhu, G. Thareja, and J. C. Lee, IEEE Electron Device Lett. **27**, 145 (2006).
[9]R. L. Puurunen, J. Appl. Phys. **97**, 121301 (2005).
[10]C. L. Hinkle, A. M. Sonnet, E. M. Vogel, S. McDonnell, G. J. Hughes, M. Milojevic, B. Lee, F. S. Aguirre-Tostado, K. J. Choi, H. C. Kim, J. Kim, and R. M. Wallace, Appl. Phys. Lett. **92**, 071901 (2008).
[11]V. Malhotra and C. W. Wilmsen, in *Handbook of Compound Semiconductors: Growth, Processing, Characterization, and Devices*, edited by P. H. Holloway and G. E. McGuire (Noyes, New Jersey, 1995), pp. 328–335.
[12]K. Martens, W. Wang, K. De Keersmaecker, G. Borghs, G. Groeseneken, and H. Maes, Microelectron. Eng. **84**, 2146 (2007).
[13]C. J. Sandroff, R. N. Nottenburg, J.-C. Bischoff, and R. Bhat, Appl. Phys. Lett. **51**, 33 (1987).
[14]E. Yablonovitch, C. J. Sandroff, R. Bhat, and T. Gmitter, Appl. Phys. Lett. **51**, 439 (1987).
[15]R. N. Nottenburg, C. J. Sandroff, D. A. Humphrey, T. H. Hollenbeck, and R. Bhat, Appl. Phys. Lett. **52**, 218 (1988).
[16]H. Sugahara, M. Oshima, H. Oigawa, H. Shigekawa, and Y. Nannichi, J. Appl. Phys. **69**, 4349 (1991).
[17]Z. H. Lu, M. J. Graham, X. H. Feng, and B. X. Yang, Appl. Phys. Lett. **62**, 2932 (1993).
[18]H. Sik, Y. Feurprier, C. Cardinaud, G. Turban, and A. Scavennec, J. Electrochem. Soc. **144**, 2106 (1997).
[19]T. Ohno, Phys. Rev. B **44**, 6306 (1991).
[20]D. Shahrjerdi, E. Tutuc, and S. K. Banerjee, Appl. Phys. Lett. **91**, 063501 (2007).
[21]D. Shahrjerdi, D. I. Garcia-Gutierrez, E. Tutuc, and S. K. Banerjee, Appl. Phys. Lett. **92**, 223501 (2008).
[22]P. D. Ye, G. D. Wilk, B. Yang, J. Kwo, S. N. G. Chu, S. Nakahara, H.-J. L. Gossmann, J. P. Mannaerts, M. Hong, K. K. Ng, and J. Bude, Appl. Phys. Lett. **83**, 180 (2003).
[23]M. M. Frank, G. D. Wilk, D. Starodub, T. Gustafsson, E. Garfunkel, Y. J. Chabal, G. Grazul, and D. A. Muller, Appl. Phys. Lett. **86**, 152904 (2005).
[24]C. J. Sandroff, M. S. Hedge, L. A. Farrow, C. C. Chang, and J. P. Harbison, Appl. Phys. Lett. **54**, 362 (1989).
[25]C. J. Powell and A. Jablonski, NIST Electron Effective Attenuation-Length Database Version 1.1, NIST Standard Reference Database 82.
[26]J. Spindt, D. Liu, K. Miyano, P. L. Meissner, T. T. Chiang, T. Kendelewicz, I. Lindau, and W. E. Spicer, Appl. Phys. Lett. **55**, 861 (1989).